Classification with Random ForestBased onLocal Tangent Space Alignment and Neighborhood Preserving Embedding for MSER features: MSER_DFT_LTSA-NPE_RF

Sevcan Aytaç Korkmaz*, Furkan Esmeray**
*Fırat University / Electronic and AutomationDepartment, Elazığ, Turkey
**Munzur University / Electric and EnergyDepartment, Tunceli, Turkey

Abstract—*In this article, 180 gastric images taken with Light Microscope help are used. Maximally Stable Extremal Regions (MSER) features of the images for classification has been calculated. These MSER features have been applied Discrete Fourier Transform (DFT) method. High-dimensional of these MSER-DFT feature vectors is reduced to lower-dimensional with Local Tangent Space Alignment (LTSA) and Neighborhood Preserving Embedding (NPE). When size reduction process was done, properties in 5, 10, 15, 20, 25, 30, 35, 40, 45, and 50 dimensions have been obtained. These low-dimensional data are classified by Random Forest (RF) classification. Thus, MSER_DFT_LTSA-NPE_RF method for gastric histopathological images have been developed. Classification results obtained with these methods have been compared. According to the other methods, classification results for gastric histopathological images have been found to be higher.*

Keywords—*Maximally Stable Extremal Regions; Neighborhood Preserving Embedding; Local Tangent Space Alignment; Random Forest*

I. INTRODUCTION

Stomachcancer is a type of cancerthatoccurs in theStomachcancer, StomachtissueandStomachwall. AccordingtostudiesconductedbytheMinistry of Health, Stomachcancerwasidentified as thesecondmostcommoncancertype. Endoscopy is themostimportantfactor in theearlydiagnosis of thisdisease. Endoscopicexamination of theendometriumandbiopsyspecimensaretakenanddi agnosed as pathologicalexaminations. It is seenthathalf of thepeoplewhohavethisdiseasearelate in thediagnosisanddoctorscannotapplyanytreatment [1,2]. Themostcommonsites of thisdisease in theworldaredistantcountriessuchas Japan andChina.Japan, thenumber of peoplewithStomachcanceraccountsforabout 30% of othercancerdiseases. IntheAmericas, thenumber of Stomachcancerpeopleincreaseseveryyear [1,3-4].Accordingtoresearchconductedworldwide, 26% of malesand 11% of femaleshaveStomachcancer. Stomachcancer is located in thethirdplaceafterlungandbreastcancer in womenandsecondplaceafterlungcancer in males. Accordingtothenumber of newStomachcancer is estimatedto be around 30 thousand a year [1,5].S. Yoshihiro and colleagues [6] studied Stomach cancer by developing computer-based systems that can predict the risk factor. In the system developed, endoscopy images were taken from patients carrying H. pylori bacteria. 15 parameters were used to classify the Stomachmucosa with 3 parameters on the back panel. The classification data were processed by Bayesian theorem and outputs were obtained. This study is the source for the treatment of patients who are at risk of Stomach cancers or patients who have to undergo endoscopy [1]. D.Ahmadzadeh [7] developed a cancer diagnosis system by using KDM (decision support machine) and local pattern algorithm methods for Stomach cancer diagnosis. By using the feature identification, feature extraction and noise reduction steps in the system they have developed, the results of estimation of 91,8% of 55 randomly selected samples were found. The common feature of both systems used in the study is that it is a system that helps the doctor in time andmaterial sense [1].Akbari et al. [8] developed a Stomach cancer diagnosis system by using infrared ultra-spectral imaging method. This study was performed by selecting patients with Stomach cancer. Spectral features were extracted from cancerous and normal tissues and compared with this, KDM method was used to determine the detection of cancerous regionsbyspectraldiagramItwasperformed.High performancewasobtained from the system by using HFD and Log transformation in the direction of the obtained data. In the study performed, 25 patients with indole cancer were detected in 30 patients and 83,3119% of the obtained system was mathematically successful [1]. Stomach cancer is a type of cancer that, when diagnosed late, leads the patient todeath [1, 9].Stomachcancerusuallybeginswith ulcer and

gastritis complaints. Cancer can affect lymph nodes and other peripheral organs [1,10].

Methods of thestudyaregiven in Section 2. Experiment resultsaredescribed in Section 3. Discussionsaredescribed in Section 4, andconclusionsareexplained in Section 5.

Thepurpose of thisarticle is toadd a differentstudytotheliteraturetohelpearlydiagnosis of stomachcancerusingimages of histopathology.Thenovelty of thisstudy, whenstudies in theliteratureareexamined, it is seenthat MSER, DFT, LTSA, NPE and RF methodsare not used together to help diagnose early gastric cancer.Wehave put forward a more powerful computer-aided method of using these methods together in thesame moment. Also, the classification performances have been compared according to the number of selected MSER features.

II. THEORY AND METHOD

A. Maximally Stable Extremal Regions (MSER)

The MSER algorithm is an algorithm used to find circles or ellipse-like shapes (blobs) in images. The algorithm selects key points taking these shapes into account and calculates their attributes on these key points [11].An MSER region [12] consists of a set of interconnected points over a certain threshold value, whose persistence is dependent on the changing threshold value. In other words, the selected region is a local binary form that does not depend on a set of threshold values. According to the study given in Reference [13], finding MSER regions works in a similar way to the Watershedding method. The threshold value is changed to vary between [0-255], while regions connected to one another, which do not change or change very little in all scenes, are called as MSER regions.

In the implementation of the method; the image points are sorted by the brightness value. and the points are placed in the image in ascending or descending order. During this process, the component regions and fields is kept in a list by finded with the join detection algorithm. At each step of the thresholding process, the small region with the association of the two regions is included in the large region. and the smaller region is removed from the list. The threshold values at which the variation of the zone area is minimized by increasing / decreasing the threshold value are selected as the threshold ranges producing the maximum stable extremal zones. In other words, the boundaries of the end regions formed by the connected components at all threshold values are represented as$Q_1, \dots Q_{i-1}, Q_i, \dots$ a series of contiguous regions. This sequence provides the $Q_i \subset Q_{i+1}$ condition. In order to select the $Q_i{}^*$extremal region of the array as the maximum stable [13]; To be local minimum is required in i^* value of the $q(i) = |Q_i \pm \Delta|/|Q_i|$ expression. In this expression, $|.|$ denotes the area of the region, and Δvalue denotes a parameter of the method. The $\pm$ sign also indicates that there are local minimum for both decreasing and increasing threshold values. This process is applied on all the region arrays in the set of extremal regions to obtain the maximum extremal stable regions [13].

In the MSER method, neighboring image points having a similar color are subjected to clustering based on the stacked clustering. For clustering process, the color distances of four or eight neighboring points to one another are kept at an associated list. At each step of the algorithm, $t \in [0 \dots T]$, the image points are labeled progressively. If the coordinate space of the image points is denoted as a set of labels $\Omega = [1 \dots L]x[1 \dots M] \subset Z^2$, each step is expressed as $E_t: \Omega \rightarrow$ N mapping. As a result of the labeling, the connected points with the same indicate specify the image extremal regions. The distance between all neighboring points of the image extremal region must be lower than $d_{thr}(t)$, which is a threshold value calculated for the step in question. The distance of the image points in the color space is calculated using the chi-square distance. Initially, all values in the E_0label image are labeled as 0. In $E_t$tag image, all neighbor points with a distance less than $d_{thr}(t)$ are labeled as new region and E_{t+1}tag image is obtained [13]. Due to the spatial relationship between the image points, the distances of all neighboring points do not show a uniform distribution. The vast majority of distances have small values, and large distance values in very few number exist. Therefore, at each step, the threshold value is increased linearly, resulting in a very rapid number of tag changes at the beginning. Thus, to the end of the steps, the labels of many points change [13]. In order to change the label of an equal number of image points in each step, the distance between all neighboring points in the image is taken as a random variable and the threshold values are modified according to the ordered reversal of the cumulative distribution function (CDF) of this random variable [13]. The chi-square CDF for colored images is calculated as in Equation (1)

$$C_3(x) = \sqrt{\frac{4x}{\lambda\pi}} e^{-3x/2\mu} + erf\left(\sqrt{3x/2\mu}\right) (1)$$

where μ is the mean of the sample set. As a result, Equation (2) is used to find the threshold values after the average estimate.

$$d_{thr}(t) = c^{-1}\left(\frac{t}{T}\right) \qquad t \in [0 \ldots T] \qquad (2)$$

Next, field changes of the extremal regions detected by increasing the value of $d_{thr}(t)$at each step are checked. and maximum stationary ones are detected. In addition, those smaller than a given value are eliminated from the maximum stableextremal regions [13].

B. Discrete Fourier Transform (DFT)

Fourier transformation is a mathematical method that allows a periodic signal to be expressed by sinus and cosine components at different frequencies [14]. The Fourier transformation is defined for an array of infinite lengths, and more importantly, a function of the *w* angular frequency, which is a continuous variable. When using MATLAB, we do not limit arrays and we need to evaluate for a limited number of points. Discrete Fourier Transform (DFT) eliminates these problems. In this article, a discrete Fourier transform (DFT) of multidimensional MSER property values is calculated using a Fast Fourier Transform (FFT) algorithm. The discrete Fourier transform is expressed as follows

$$X(k) = \sum_{n=0}^{N-1} x(n) W_N^{nk} \; 0 \le k \le N-1 \qquad (3)$$

where is $W_N = e^{-j\left(\frac{2\pi}{N}\right)}$. if the *N* sequence length is large, the direct presence of the DFT requires a large amount of processing. That is, as the *N* number increases, the number of transactions made increases rapidly and the number of transactions goes to an unacceptable level. In 1965, Cooley and Tukey developed a procedure to reduce the amount of processing required for Discrete Fourier Transform [14]. This procedure caused a sudden increase in DFT applications in digital signal processing and other fields. It has also been a pivotal step in the development of other algorithms. All these algorithms are known as Fast Fourier Transform (FFT) algorithms. These algorithms have greatly reduced the number of operations required for the DFT account, thereby ensuring ease of operation. FFT is an efficient and economical algorithm for DFT computation [15].

C. Local Tangent Space Alignment (LTSA)

Given A m-dimensionalpointssampledpossiblywithnoisefrom an underlying d-dimensionalmanifold, thisalgorithmproduces A dimensionalcoordinatesTϵR^{dxn} for the manifold constructed from f localnearestneighbors [16].

Step 1. Extractinglocalinformation:
Foreach a = 1, · · · ,A,Determine f nearestneighborsx_{ab} of x_a, b = 1, . . . ,f.Computethe d largesteigenvectorseigenvectors$g_1,\ldots,g_d$ of the correlation matrix $(X_a - {}^{-}x_a e^T)^T (X_a - {}^{-}x_i e^T)$, and set

$$G_a = [e/\sqrt{f}, g\_1, \cdots, g\_d] \qquad (4)$$

Step 2. Creation of thealignmentmatrix: If a directeigenvaluedecomposition is used, createthealignmentmatrixΦaccordingtothelocalcollection. Otherwise, apply a routinethatcomputesthematrix-vectormultiplicationfor an arbitraryvector$u$[16].

Step 3. Calculatethesphericalcoordinates: Calculatethesmallesteigenvector of d + 1 andselecttheeigenvectormatrix$[u_2, \cdots, u_{d+1}]$correspondingtothesmallesteigenvalues, and$T = [u_2, \cdots, u_{d+1}]^T$[16].

D. Neighborhood Preserving Embedding (NPE)

Neighborhood Preserving Embedding (NPE) is a linear approach to the LLE algorithm [17].Thealgorithmicprocedure is formallydescribedbelow:

1. ***Constructing an adjacencygraph****:*Let'sshow a graphwith G, m nodes. The i-thnodecorrespondstothe$a_i$datapoint.Therearetwoa ystocreate an adjacencygraph. [17]:
• K nearestneighbors:Put an edgeorientedfromnode itoj if$a_u$is amongtheKnearestneighbors of a_i.
• ϵ neighborhood:uif $\|a_u - a_i\| \le \epsilon$andPut an edgebetweennodesi.

Thegraphicgeneratedbythefirstmethod is a graphic, built in thesecondmethod a non-directionalgraph. It is difficulttochoose a goodϵ in manyrealworldapplications.That's it,thegraphweadoptthe knnmethodtocreatesimilarity.

2. ***Computing theweights****:*Inthis step, theweights at theedgeshavebeencalculated.LetWdenotetheweight matrixwithW_{iu}havingtheweight of theedgefromnode$i$tonode$u$, and 0 if there is no such edge. The weights on the edges can be calculated by minimizing the following objective function [17],

$$min \sum_i \|a_i - \sum_u w_{iu} a_u\| \qquad (5)$$

withconstraints

$$\sum_u w_{iu} = 1, u=1,2,\ldots,m \qquad (6)$$

3. ***Computing theProjections:*** Inthis step, thelinearprojectionshavebeencalculated. Solvethefollowinggeneralizedeigenvector problem [17]:

$$AKA^{T}a = \lambda AA^{T}a \quad (7)$$

where

$$A = (a_1, \cdots, a_m)$$

$$K = (Im - W)T\,(Im - W)$$

$$Im = diag(1, \cdots, 1) \quad (8)$$

It is easytocheckthatKis symmetric. Letthecolumnvectors$x_o, \cdots, x_{d-1}$be thesolutions of Equation (9), orderedaccordingtotheireigenvalues, $\lambda 0 \leq \cdots \leq \lambda d - 1$. Thus, the embedding is as follows:

$$a_i \rightarrow y_i = A^T a_i$$

$$X = (x_o, \cdots, x_{d-1}) \quad (9)$$

where*d*-dimensionalvector is y_i,and*X*is an $n \times d$matrix.

E. Random Forest (RF)

RF is a collection of tree type classifiers. The Gini index is used in RF classifier. The division position according to the smallest Gini index is determined by Gini measurements. To generate a tree with the RF classifier, two external parameters must be entered. These parameters are *m* and *N* parameters. *m* is the number of variables used in each node. *N* is the number of trees that will be developed to determine the best partition [18,19]. The start m value is entered randomly from the outside. Subsequent *m*'s are reduced or increased relative to the overall error rate. Classification accuracy is understood by generalized error data. *P* new training data is generated from *R* training data. Tree-type classifiers in the RF classifier are used in the $\{h(x, \theta_P)P = 1, \ldots\}$ type. where, *x* is the input data; θ_P indicates the random vector. The $h(x, R_P)$ classifier is constructed using the new training data set. The *x* and *y* are not found in R_k. When a random pixel is selected for a given training data set R, this pixel belongs to class S_i.Therefore, the Gini index is expressed as below.

$$\sum\sum_{j \neq i} (f(S_i, R)/|R|)(f(S_j, R)/|R|) \quad (10)$$

Here, R is the training data set,S_i is the class to which a randomly selected pixel belongs, $f(S_i, R)/|R|)$ indicates the possibility of belonging to the S_i class of the selected example.

In this article has been used the MSER features. The dimensions of these features have been reduced to lower dimensions with help the DFT-LTSA, and DFT-NPE methods by the Linear Discriminant Analysis (LDA) method. These lower size features have been classified by Random Forest (RF) method. The steps of this article are shown in Fig. 1.

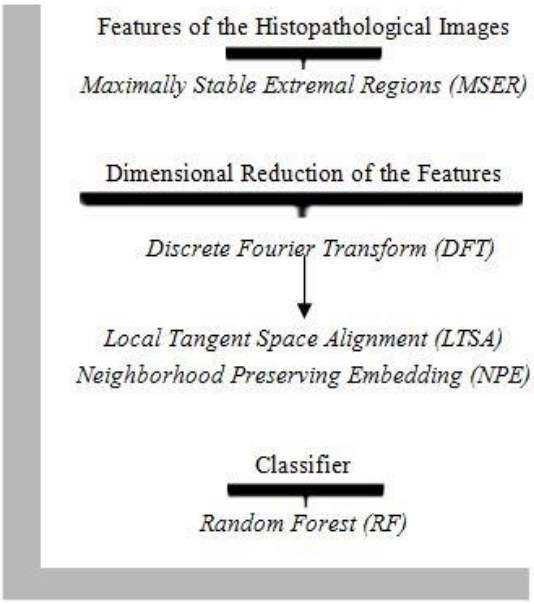

Figure 1. StepstoApply of the MSER_DFT_LTSA-NPE_RF Algorithms

III. EXPERIMENTAL RESULTS AND DISCUSSION

MSER features of stomachhistopathologyimageswerefound.Thedimensions of the MSER propertiesforeachimageareveryhighandhavebeenobtaineddifferently.Ittakes a long time toprocesswith MSER characteristicswhicharedifferentfromeachotherandveryhighdimensions. Byapplyingthe DFT methodtothe MSER featuresobtainedfromthisaspect, thecellsobtainedforthe MSER

featuresareconvertedintovectors, andthesame size valuesareobtainedforalltheimages.

TABLE 1. EXAMPLES OF DİFFERENT DİMENSİONAL CELLS FOUND FOR MSER FEATURES

MSER cellsfor normal images	MSER cellsforbenignimages	MSER cellsformalignimages
52800x1	98944x1	66944x1
34368x1	56000x1	70464x1
59776x1	41984x1	74560x1
60544x1	30656x1	81856x1
54016x1	38976x1	73600x1
46016x1	83072x1	65344x1
51712x1	80256x1	60416x1
52480x1	35264x1	54784x1
53184x1	24704x1	51712x1
48192x1	30528x1	55744x1
50432x1	41920x1	81280x1
39488x1	78912x1	124288x1
52544x1	43520x1	80960x1
75904x1	34688x1	112768x1
63872x1	53248x1	121088x1
58304x1	43520x1	94080x1

As shown in Table 1, thenumber of MSER propertiesobtainedforeachimage is differentfromeachother.Wehaveappliedthe DFT methodtotheseobtainedpropertyvalues becausethenumbers of thesepropertiesaredifferentforeachimage.

Whenthe DFT method is applied, thefeature size obtainedfor normal images is 60x183680.It is 60x197888 forbenignimages.60x379008 formalignimages.Finally, LTSA and NPE size reductionmethodswereappliedtofeaturevalues of theseimages.Featurevalues of 5, 10, 15, 20, 25, 30, 35, 40, 45, 50 for LTSA and NPE size reductionmethodswerediscussedrespectively. 30 normal + 30 benign + 30 malignimageswereusedfortestingpurposeswhile 180 imageswereusedfor 30 normal + 30 benign + 30 maligneducationalpurposes.Andthe test imageswereclassifiedwiththerandomforestclassifier. Accordingtothefeaturenumbersselected in Table 2, theclassificationperformancesobtainedwiththe RF classifierareshown.AccordingtoTable 2Thehighestclassificationperformanceobtainedwith LTSA is 94.44%. Thisratiowasobtainedbyselecting 15 properties.However, thehighestclassificationperformanceobtainedwith NPE is 86.66%.Thisratiowasobtainedbyselecting 10 properties.Based on theseresults, the LTSA size reductionmethodoverthe MSER_DFT propertyvalues showedhigherclassificationperformancethanthe NPE size reductionmethod.As shown in Table 1, boththe LTSA andtheNPE'sclassificationperformancedecreases as thenumber of featuresincreases.This is shown in thegraphic in Figure 2.

TABLE 2. CLASSIFICATION PERFORMANCES OF RF CLASSİFİER ACCORDİNG TO SELECTED FEATURE NUMBER

ClassificationPerformances (%)										
SelectedFeatureNumber	5	10	15	20	25	30	35	40	45	50
MSER_DFT_LTSA_RF	92.22	91.11	94.44	87.77	88.88	82.22	77.77	68.88	54.44	46.66
MSER_DFT-NPE_RF	84.44	86.66	81.11	76.66	66.66	65.55	56.66	50.00	53.33	47.77

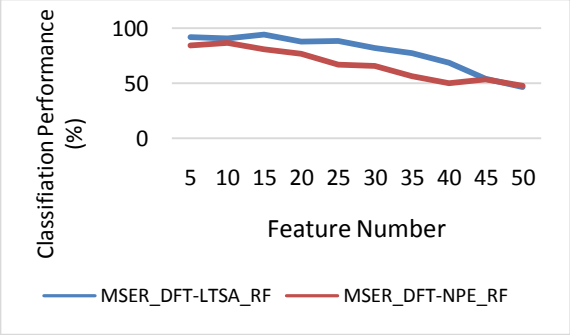

Figure 2. Comparison of theClassificationPerformancesfoundwith MSER_DFT_LTSA_RF and MSER_DFT_NPE_RF Algorithms

InTable 3, GLCM is Gray Level Co-occurenceMatrixFeatures. LBP is LocalBinaryPatternsFeatures. LPP is LocalityPreservingProjectionsfordimensionalreduction. HOG is Histograms of OrientedGradientFeature. LDA is LinearDiscriminant Analysis. ANN isArtificialNeural Network.

InTable 3, HOG_LDA_ANNaccuracy rate wasfound as 88,9 %. LBP_LPP_ANN accuracy rate wasfoundas 85.56 %. GLCM_LPP_ANNaccuracy rate wasfoundas 80.12%. OurMethod MSER_DFT_LTSA_RF accuracy rate has beenfound as 94.44%.

TABLE 3. COMPARİSON OF DİFFERENT RESULTS

Compared	
Method	Accuracy
Our Method MSER_DFT_LTSA_RF	94.44 %
Our Method MSER_DFT_NPE_RF	86.66 %
HOG_LDA_ANN [1]	88,9 %.
GLCM_LPP_ANN [1]	80.12 %
LBP_LPP_ANN [20]	85.56 %

IV. CONCLUSION

Untiltoday, manyclassificationmethodshavebeenused in thefield of health [21-33].180 gastricimagestakenwithLightMicroscopehelpin thisarticlehavebeenclassified. MaximallyStableExtremalRegions (MSER) features of theimagesforclassification has beencalculated. These MSER featureshavebeenappliedDiscreteFourierTransform (DFT) method. High-dimensional of these MSER-DFT featurevectors is reducedtolower-dimensionalwithLocalTangent Space Alignment (LTSA) andNeighborhoodPreservingEmbedding (NPE). When size reductionprocesswasdone, properties in 5, 10, 15, 20, 25, 30, 35, 40, 45, and 50 dimensionshavebeenobtained. Theselow-dimensionaldataareclassifiedbyRandomForest (RF) classification. Thus, MSER_DFT_LTSA-NPE_RF methodforgastrichistopathologicalimageshavebeen developed.

Thehighestclassificationperformanceobtainedwith LTSA is 94.44%. Thisratiowasobtainedbyselecting 15 properties. However, thehighestclassificationperformanceobtainedwith NPE is 86.66%. Classificationresultsobtainedwiththesemethodshave beencomparedwithotherclassificationresults in theliterature. Accordingtotheothermethods, ourclassificationresultsforgastrichistopathologicali mageshavebeenseento be higher.Infuturestudies, an analysiswill be performedbyapplyingdifferentfeatureextractionmet hodstodifferentcancerimages.

Acknowledgements

The authors would like to thank to Prof. Dr. İbrahim Hanifi ÖZERCAN in the pathology department of the Fırat University Hospital.

REFERENCES

[1] KORKMAZ, Sevcan Aytaç, et al. A expert system for stomach cancer images with artificial neural network by using HOG features and linear discriminant analysis: HOG_LDA_ANN. In: Intelligent Systems and Informatics (SISY), 2017 IEEE 15th International Symposium on. IEEE, (2017):000327-000332.

[2] Lambert, R., Guilloux, A., Oshima, A., Pompe-Kirn, V., Bray, F., Parkin, M., Ajiki,W., Tsukuma, H. (2002). Incidence and mortality from Stomach cancer in Japan,Slovenia and the USA. *International Journal Of Cancer*,97, 811–818.

[3] Hirayama, Akiyoshi, et al. "Quantitative metabolome profiling of colon and Stomach cancer microenvironment by capillary electrophoresis time-of-flight mass spectrometry." Cancer research 69.11 (2009): 4918-4925.

[4] Brenner, Hermann, Dietrich Rothenbacher, and Volker Arndt. "Epidemiology of Stomach cancer." Cancer Epidemiology: Modifiable Factors (2009): 467-477.

[5] Fujioka, N., Morimoto, Y., Arai, T., Kikuchi, M. (2004). Discrimination betweennormal and malignant human Stomach tissues by Fourier transform infraredspectroscopy. *Cancer Detection and Prevention*, 28(1), 32–36.

[6] Yoshihiro, S., Ryukichi, H., Tetsuro Y., Norihiro H., Tatsuya M. et al. (2010).Computer-aided estimation for the risk of development of Stomach cancer by imageprocessing. *Artificial Intelligence in Theory and Practice III*, 331, 197-204.

[7] Ahmadzadeh, D., Fiuzy, M., Haddadnia, J. (2013). Stomach Cancer Diagnosis by Using a Combination of Image Processing Algorithms, Local Binary Pattern Algorithm and Support Vector Machine.*Journal of Basic and Applied ScientificResearch*, 3(2), 243-251.

[8] Akbari, H., Uto, K., Kosugi, Y., Kojima, K., Tanaka, N. (2011). Cancer detection using infrared hyperspectral imaging.*The Official Journal of The Japanese CancerAssociation*, 102(4), 852-857.

[9] Tannapfel, A., Schmelzer, S., Benicke, M. et al. (2001). Expression of the p53 homologues p63 and p73 in multiple simultaneous Stomach cancer. *The Journal ofPathology*, 195, 163–170.

[10] Onishi, Katsunori, Tetsuya Takiguchi, and Yasuo Ariki. "3D human posture estimation using the HOG features from monocular image." *Pattern Recognition, 2008. ICPR 2008. 19th International Conference on*. IEEE, 2008.

[11] Matas, J., Chum, O., Urban, M., Pajdla, T., Robust wide-baseline stereo from maximally stable extremal regions, *British Machine Vision Conference*, s.384-393, 2002.

[12] J. Matas, O. Chum, M. Urban, ve T. Pajdla, "Robust wide-baseline stereo from maximally stable extremal regions," *Image and vision computing*, Sayı 22, 761-767, 2004

[13] Güney M., Arıca N..; " Desen Tabanlı İlgi Bölgesi Tespiti" Journal of Naval Science and Engineering 2009, Vol. 5 , No.1, pp. 94-106

[14] Cooley, J.W., Tukey, J.W., An Algorithm for the Machine Computation of Complex Fourier Series, Mathematics of Computation, Vol. 19, pp. 297-301, April 1965.

[15] http://web.itu.edu.tr/~baykut/lab/pdf/Deney_3.pdf

[16] http://www.math.pku.edu.cn/teachers/yaoy/Spring2011/lecture11_2.pdf

[17] He, X., Cai, D., Yan, S., & Zhang, H. J. (2005, October). Neighborhood preserving embedding. In Computer Vision, 2005. ICCV 2005. Tenth IEEE International Conference on (Vol. 2, pp. 1208-1213). IEEE.

[18] Pal, Mahesh. "Random forest classifier for remote sensing classification." *International Journal of Remote Sensing*, vol. 26, no. 1, pp. 217-222, 2005.

[19] Korkmaz, Sevcan Aytaç, and Hamidullah Binol. "Analysis of Molecular Structure Images by using ANN, RF, LBP, HOG, and Size Reduction Methods for early Stomach Cancer Detection."*Journal of Molecular Structure* (2017).

[20] Korkmaz, S. A. (2018). LBP Özelliklerine Dayanan Lokasyon Koruyan Projeksiyon (LPP) Boyut Azaltma Metodunun Farklı Sınıflandırıcılar Üzerindeki Performanslarının Karşılaştırılması. Sakarya University Journal of Science, 22(4), 1-1.

[21] Korkmaz, S. Aytac, and Mustafa Poyraz. "A New Method Based for Diagnosis of Breast Cancer Cells from Microscopic Images: DWEE--JHT." Journal of medical systems 38.9 (2014): 1.

[22] Korkmaz, Sevcan Aytac, and Mustafa Poyraz. "Least square support vector machine and minumum redundacy maximum relavance for diagnosis of breast cancer from breast microscopic images." Procedia-Social and Behavioral Sciences 174 (2015): 4026-4031.

[23] Korkmaz, Sevcan Aytac, and Mehmet Fatih Korkmaz. "A new method based cancer detection in mammogram textures by finding feature weights and using Kullback–Leibler measure with kernel estimation." Optik-International Journal for Light and Electron Optics 126.20 (2015): 2576-2583.

[24] Korkmaz, Sevcan Aytac, Mehmet Fatih Korkmaz, and Mustafa Poyraz. "Diagnosis of breast cancer in light microscopic and mammographic images textures using relative entropy via kernel estimation." Medical & biological engineering & computing 54.4 (2016): 561-573.

[25] KORKMAZ, Sevcan Aytac; EREN, Haluk. Cancer detection in mammograms estimating feature weights via Kullback-Leibler measure. In: Image and Signal Processing (CISP), 2013 6th International Congress on. IEEE, 2 (2013):1035-1040.

[26] KORKMAZ, Sevcan AYTAÇ. "DETECTING CELLS USING IMAGE SEGMENTATION OF THE CERVICAL CANCER IMAGES TAKEN FROM SCANNING ELECTRON MICROSCOPE." The Online Journal of Science and Technology-October 7.4 (2017).

[27] KORKMAZ, Sevcan Aytaç, et al. Recognition of the stomach cancer images with probabilistic HOG feature vector histograms by using HOG features. In: Intelligent Systems and Informatics (SISY), 2017 IEEE 15th International Symposium on. IEEE, (2017). p. 000339-000342.

[28] Korkmaz, Sevcan Aytac, et al. "Diagnosis of breast cancer nano-biomechanics images taken from atomic force microscope." Journal of Nanoelectronics and Optoelectronics 11.4 (2016): 551-559.

[29] Korkmaz, S. A., Poyraz, M., Bal, A., Binol, H., Özercan, I. H., Korkmaz, M. F., & Aydin, A. M. (2015). New methods based on mRMR_LSSVM and mRMR_KNN for diagnosis of breast cancer from microscopic and mammography images of some patients. International Journal of Biomedical Engineering and Technology, 19(2), 105-117.

[30] Sengur, Abdulkadir. "Support vector machine ensembles for intelligent diagnosis of valvular heart disease." Journal of medical systems 36.4 (2012): 2649-2655.

[31] A. Şengür, "An expert system based on principal component analysis, artificial immune system and fuzzy k-NN for diagnostic of valvular heart diseases" Computers in Biology and Medicine 38 (2008) 329 – 338.

[32] Sengur, Abdulkadir, Ibrahim Turkoglu, and M. Cevdet Ince. "Wavelet packet neural networks for texture classification." Expert systems with applications 32.2 (2007): 527-533.

[33] Sengur, Abdulkadir. "Multiclass least-squares support vector machines for analog modulation classification." Expert Systems with Applications 36.3 (2009): 6681-6685.